21st Australasian Fluid Mechanics Conference
Adelaide, Australia
10-13 December 2018

Modelling the Effects of pH on Subsurface Microbial Growth Processes

S.A. Masum[1] and H.R. Thomas[1]

[1]Geoenvironmental Research Centre, School of Engineering

Cardiff University, Cardiff CF24 3AA, Wales, UK

Abstract

Subsurface microbial processes can be harnessed for a wide range of useful geo-engineering and geo-energy applications. On that regard, a coupled numerical model has been developed under a Thermo-Hydro-Chemical-Mechanical (THCM) framework including subsurface microbial processes and associated bio-geochemical reactions. In this work, the model has been used to investigate the effect of pH on biofilm growth of two bacterial species and the consequent impacts on porous media flow properties *i.e.* porosity and permeability. The processes have been investigated in both single-phase and two-phase flow. Microbial activities significantly influenced by pH, as it regulates the ionization state of a system. Microbial cell-enzymes contain ionizable groups which need to be in appropriate ionic state to bind substrates and grow biomass. The effect of pH on a medium containing either a mixed species biofilm or a mono-species biofilm has been observed over a dynamic pH condition. The results suggest that a mixed bacterial species biofilm that covers a wide range of pH activity would be ideal for bio-barrier applications. Otherwise, if a single species is chosen which is active within a specific pH range will be dormant if the pH is not in favourable regime.

Introduction

In the subsurface environment, microorganisms such as, bacteria mainly exists as suspended cells in soil porewater and as biofilms attached to soil particles. Biofilms are microbial populations, encapsulated in their self-produced extracellular polymeric substances (EPS) and attached to solid surfaces (Bakke, 1986; Mitchell et al., 2009). Biofilms are often known for their negative or detrimental effects in industrial, medical (Phillips et al., 2013) and engineering applications. Biofilms causes biofouling or bio-clogging which affects flow processes. However such properties can also be adopted for useful engineering applications. For example, deep geological sequestration of anthropogenic carbon dioxide in saline aquifers or un-mineable coal seams is an important strategy to reduce global greenhouse impacts. Subsurface biofilms are effective in enhancing carbon dioxide trapping mechanisms and limiting the leakage of sequestered supercritical carbon dioxide through geologic cap-rocks, formation fractures and near the injection wells (Mitchell et al., 2009; Masum and Thomas, 2018). Therefore, usage of biofilms as bio-barriers or to enhance the performance of geological and engineered barrier systems could be significantly beneficial. However, better understanding of fundamental behaviours and key microbial processes are essential to ensure successful and efficient applications.

Bacteria and/ biofilms mainly grow by metabolising suitable growth substrates either in presence or in absence of electron acceptors. The growth kinetics are influenced by the pH of the local environment (Ibragimova et al., 1969; Tan et al., 1998; Hoštacká et al., 2010; Masum and Thomas, 2018). The growth of certain microbes have been reported to occur in acidic conditions, whereas the others preferably in neutral to alkaline conditions. pH influences the ionization state of the components in a system (Dixon and Webb, 1979). The active components of microbial cells are usually the cell-enzymes (Tan et al., 1998). Enzymes contain ionizable groups those should be in appropriate ionic states to bind with growth substrates, to catalyze relevant reactions, and to produce biomass (Segel, 1975). Hence, for a particular species to be effective as a bio-barrier, ideal pH condition should be ensured. Otherwise, a shift in pH level might hinders growth and its sealing/clogging properties.

An alkaline environment is preferred for carbon sequestration techniques, nevertheless continuous injection of supercritical carbon dioxide may shift the environment to acidic conditions. Biofilm species which is preferred as the potential barrier could become ineffective in such circumstances. In subsurface these processes are complex and coupled with multiples phases, flows, reactions and stress conditions. To study the complex interactions or processes Masum and Thomas (2018) presented a microbial model which was developed under a coupled THCM framework. The model deals with liquid flow, multicomponent gas flows, dissolved chemicals and suspended microbes flows in liquid phase, heat flow, biofilms and minerals growths, mechanical deformations and geochemical/bio-geochemical reactions. In addition, the multicomponent feature of the model allows to investigate multiple species or community interactions. In this paper the model has been used to investigate effect of pH on the growth kinetics of two biofilm species and the consequent impact on their bio-barrier performance *i.e.* reducing system porosity and permeability. One of them is considered to prefer alkaline environment, while the other an acidic media. In the simulations, carbon dioxide has been injected in a partially saturated porous medium and it dissolved in the porewater to influence pH of the medium. Performance of a mixed biofilm (combination of two species) as well as a single biofilm, under such conditions, has been observed.

Model setup

Theoretical and numerical formulation of the coupled microbial model has been described in Masum and Thomas (2018). Governing equations, which are relevant to this paper, are presented below. To fit to the scope of the paper, following assumptions have been made: i) biofilms are impermeable and their density is constant; ii) gas transports mainly via diffusion and advection is negligible; iii) substrate concentration in the medium remains constant, despite microbial consumption. That means supply of substrate is faster than the consumption and no depletion zone is present.

The total porosity, n_0 of an unsaturated porous medium can be divided into liquid phase, gas phase and biofilm phase as,

$$\theta_l + \theta_g + \theta_b = n_0 \tag{1}$$

where θ_l, θ_g, θ_b are the volumetric liquid, gas and biofilm contents, respectively. Growing biofilms occupy void spaces and restrict overall flow processes in the medium. Therefore, porosity is affected by the biofilm phase volume and,

$$\theta_l + \theta_g = n_0 - \theta_b = n. \tag{2}$$

Here n represents active porosity which is not affected by the biofilm phase and where fluid flow processes mainly takes place.

The mass balance equation of a biofilm attached to solid surfaces is given by,

$$\frac{\partial}{\partial t}(c_b^s) = s_b^s \tag{3}$$

where c_b^s represents the amount of biofilm per unit volume of the porous media and s_b^s is the sink or source term. Biofilm concentration is related to biofilm volumetric content via $c_b^s = \theta_b \rho_b^s$, where ρ_b^s is the biofilm mass density *i.e.* the amount of dry biomass per unit wet volume of the biofilm. The sink/ source term estimates biomass accumulation via physical growth (*e.g.* substrate metabolism, attachment) or loss due to decay processes (*e.g.* endogenous decay, biocide decay, detachment, shear loss *etc*.). Also includes the influences of local geochemical condition and any external sink/ sources that might present. In this paper, only metabolic growth and endogenous/ cell death have been considered. Therefore,

$$s_b^s = r_{subs} - r_{decay} \tag{4}$$

The rate of substrate metabolism is generally expressed via Monod's equation. When the growth is limited by both substrate and electron acceptor, the process is explained by the dual Monod's kinetics as,

$$r_{subs} = k_+ \left(\frac{c_d^s}{K_s' + c_d^s}\right)\left(\frac{c_d^e}{K_e' + c_d^e}\right) c_b^s \tag{5}$$

where c_d^s represents substrate concentration and c_d^e is the concentration of electron acceptor in the liquid phase. K_s' and K_e' are Monod half-saturation constants of substrate and electron acceptor, respectively. k_+ represents substrate utilisation rate which has been considered a function of pH in this paper.

Ibragimova et al. (1969) and Tang et al. (1989) presented a pH dependent growth rate (Tan et al., 1998) as,

$$k_+ = \frac{k_0 + \frac{k_1}{K_1}[H^+]}{1 + \frac{1}{K_1}[H^+]} \tag{6}$$

Here k_0 and $k_1$are specific rates, $K_1$is a constant known as ionisation constant and $[H^+]$ is the concentration of hydrogen ion in the liquid phase. k_+ increases monotonically and reaches a constant value when k_1=0; whereas it decreases with pH and reaches to zero at high pH when k_0=0.

Loss of biomass is expressed using a first-order rate as,

$$r_{decay} = k_- c_b^s \tag{7}$$

where k_- is the endogenous cell death rate.

The governing equation of gas transport equation is given by,

$$\frac{\partial(\theta_g c_g)}{\partial t} = \nabla\left(\theta_g D_g \nabla c_g\right) + \nabla\left(\theta_g v_g c_g\right) + s_g. \tag{8}$$

Here c_g represents gas concentration *i.e.* the amount of moles of the gas in the gas phase. v_g is the gas phase advective velocity, s_g is the gas sink/source and partitioning of the gas with liquid phase is considered to be in equilibrium following Henry's law. D_g is the effective diffusion coefficient which is calculated as,

$$D_g = \tau_g D_g^0 \tag{9}$$

where D_g^0 is the diffusion coefficient of gas in free flow condition and τ_g is the gas phase tortuosity factor, which is obtained from the Millington and Quirk (1961) model as,

$$\tau_g = n^{1/3} S_g^{7/3} \tag{10}$$

where S_g is the gas saturation.

The governing equation for liquid phase flow in a multiphase system is presented as,

$$\frac{\partial(\theta_l \rho_l)}{\partial t} = \nabla(\theta_l \rho_l v_l) + s_s \tag{11}$$

where ρ_l is the density of liquid phase, v_l is the flow velocity and s_s is the sink/source term. The phase velocity terms (v_g and v_l) are calculated following Darcy's law as,

$$v_i = \frac{k_{ri} k_{int}}{\mu_i} \gamma_i \nabla\left(\frac{u_i}{\gamma_i}\right). \quad i \in \{g, l\} \tag{12}$$

Here k_{int} is the intrinsic permeability, k_{ri} relative permeability, μ_i viscosity, γ_i unit weight of the gas or liquid, u_i is the gas or water pressure.

Simulation setup

In this section the model has been applied to demonstrate the effects of pH on biofilm growth in a partially saturated porous medium. Two bacterial species, "species 1" (Sp1) and "species 2" (Sp2), with optimal growth rates at different pH levels have been considered in the simulations. Sp1 favours growth at high pH condition, whereas Sp2 prefers low pH. Firstly, two sets of simulations have been carried out to observe bio-barrier performance, (1) when the two biofilm species act simultaneously and (2) when only one of them is present, under a dynamic pH condition. The change in pH occurred due to injection and dissolution of carbon dioxide gas in the porewater. Since the space for growth is limited, when coexist, the two species compete with each other until all of the available space is fully occupied. It has been assumed that the substrate metabolism rate is not limited by any electron acceptor and therefore, $[c_d^e/(K_e' + c_d^e)] \approx 1$ in Eq.(5). Gas transports mainly via diffusion. The 0.1m by 0.01m porous medium has been discretized into 100 4-noded quadrilateral elements. The simulations have been carried out for 7 days.

In an additional simulation, the pH dependent biofilm growth has been observed under a two-phase flow condition. In this simulation a 1.0 m by 0.2 m partially saturated sandstone core has been discretized into 100 4-noded quadrilateral elements. The simulation has been carried out for 24 hrs. The presence of both biofilm species and advective-diffusive transports have been considered in this case.

Initial and boundary conditions

To begin with, it has been assumed that the concentrations of both biofilm species, Sp1 and Sp2, are 1.0 kg/m3. Substrate concentration, c_d^s=25 kg/m^3 which remains constant during the simulations. Initial gas concentration, c_g=0. The medium is 86% saturated and initial pH=8.0.

Carbon dioxide gas has been injected through the right boundary (*i.e.* x = 0.1) at the rate of 1.0×10^{-8} mol/m^2/s; whereas the left boundary (*i.e.* x = 0) is impermeable.

The initial conditions for the two-phase flow simulation are same as above and boundary conditions for the two-phase flow simulations are as follows: fixed water pressure at the right and the left boundaries $u_l|_{x=1}$ =10 and $u_l|_{x=0}$ =1 Pa, respectively. The gas has been injected through the left boundary (*i.e.* x = 0) at the rate of 1.0×10^{-8} mol/m^2/s.

Results and discussion

The simulation parameters are presented in Table 1. The results of the simulations are presented in Figures 1-4. Please note that the graphs indicating (Sp1+Sp2) represent the simulations

where both species are considered and "Sp1 only" represents the presence of just one species (Sp1) in the medium. The evolution results are plotted at x=0.05 m.

Parameters	Values	Ref
Total porosity, n_0	0.446	
Specific rate, k_0	5.42×10^{-5} s^{-1}	[14]
Specific rate, k_1	5.77×10^{-5} s^{-1}	[14]
Ionisation constant, K_1	9.04×10^{-8} mol/l	Sp1,[14]
Ionisation constant, K_1	2.73×10^{-7} mol/l	Sp2,[14]
Monod's constant, K_s'	26.9×10^{-3} kg/m^3	[2]
Cell death rate, k_-^e	3.18×10^{-7} s^{-1}	[13]
Biofilm density, ρ_b^s	65 kg/m^3	[9]
Henry's constant	3.4×10^{-4} mol/l/atm	[12]
Diffusion coeff, D_g^0	1.0×10^{-5} m^2/s	[4]

Table 1. Parameters required for the "both species" and "single species" simulations. Additional fluid flow parameters required for the two-phase flow simulation are listed in Masum and Thomas (2018).

Evolutions of pH and gas concentration associated with CO_2 injection are presented in Figure 1. The results show that the constant injection and dissolution of the gas reduces the pH of the medium from 8.0 to 5.5 within 1.4 d in "both species" simulation. In the early stages, gas pressure builds slowly since at higher pH more CO_2 dissolves in the porewater. The dissolution slows down at lower pH values and CO_2 concentration rises rapidly in the gas phase. It is noticeable that both pH and gas concentration in "both species" simulation reach to steady values after 1.4 d, which is due to maximum accumulation of biofilms (Figure 2) and reduction of the active porosity to the minimum (Figure 3). At such low porosity no flow can takes place and the whole medium behaves as an impermeable system. The solid lines in Figure 2 represents the results of biofilm accumulation when both species are considered. The results show that biofilm Sp1 grows gradually at the beginning of the simulation when pH of the medium is relatively high. The net growth of Sp2, which favours low pH, is very slow at that time but increases sharply as the pH of the medium drops. Since in the simulation elevated pH did not prevail long, the growth of Sp1 is low and Sp2 is significantly high. During the growth processes, both species competed for space. However, the growth of Sp2 dominates over Sp1 until the available space is fully occupied. The relevant porosity evolution result in Figure 3 (together with the results in Figure 2) suggest that biofilm Sp2 contributed largely in porosity reduction.

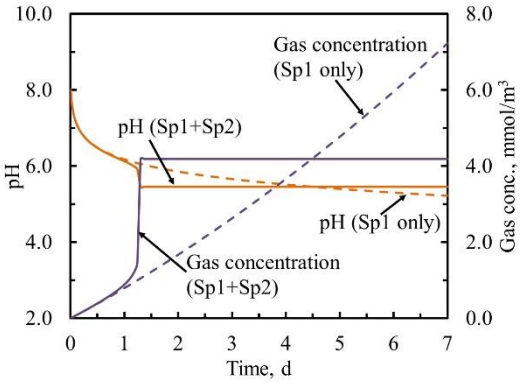

Figure 1. Evolution of pH and gas concentration in the medium (at x=0.05). *Solid-lines* and *dashed-lines* represent "both species" and "single species" simulations, respectively. (Sp1+Sp2) indicates mixed biofilm ("both species") scenario, whereas (Sp1 only) indicates single biofilm ("single species") scenario. Simulation period 7 days.

In the single species simulations, where only Sp1 is present, evolution of gas and pH in the medium is gradual (Figure 1). Since more gas has been injected than that of the "both species" simulation, the reduction of pH is slightly higher. As it can be seen that the pH, in "both species" simulations reaches to 5.5; whereas in this case to 5.2, after 7 days. More gas injection was possible since the active porosity (Figure 3) reduced to 0.25, instead of zero in "both species" scenario, during the simulation period. Net biofilm accumulation after 7 days is 13.8 kg/m^3 in comparison to 31 kg/m^3 (both species), suggesting more available pore space for flow and biofilm growth. During the "single species" simulation, the biofilm Sp1 experiences mainly low pH condition and in the time the growth slows down, as the gradient of the curve softened (Figure 2).

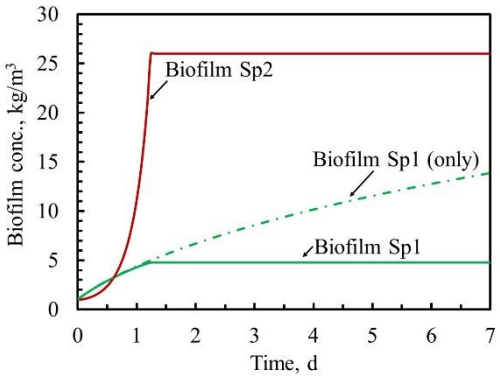

Figure 2. Biofilm growth in the medium (at x=0.05). *Solid-lines* and *dashed-line* represent "both species" and "single species" simulations, respectively.

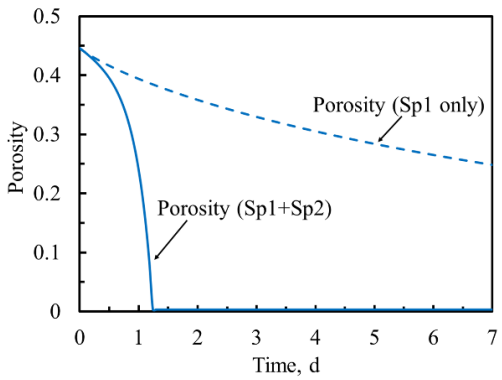

Figure 3. Evolution of porosity in the medium (at x=0.05). The *Solid-line* and *dashed-line* represent "both species" and "single species" simulations, respectively.

In Figure 4, the profiles of biofilm concentrations and porosity, for "both species" and "single species" simulations, along the length of the sample are presented. The results are plotted at the end of the simulation period. Since gas was injected from the right boundary *i.e.* x=0.1, the growth of biofilm Sp2 within the vicinity of the boundary is higher than the rest of the domain. In the medium, accumulation of biofilm Sp2 dominates over Sp1, but together they reduces the overall porosity to zero near the boundary. On the other side, the growth of Sp2 is less and consequently the reduction of porosity. Meanwhile, during the "single species" simulation, lesser amount of Sp1 accumulated in the right boundary than the rest of the medium. Porosity reduction is less in this area in comparison to the rest of the domain.

In Figure 5, the results of two-phase flow simulation are presented. The results show that the liquid saturation increases sharply at the vicinity of the water boundary. CO_2 transports through the unsaturated region and increases the concentration. Dissolution of CO_2 in the porewater reduces the pH near the gas injection face. This is therefore influences the bacterial growth

across the length of the sample. Growth of Sp1 occurs mainly at the region beyond the CO_2 augmented zone where pH is relatively high. However, Sp2 growth is significant at the augmented zone where pH is relatively low. The results demonstrate the effects of simultaneous liquid flow and gas flow on pH dependent microbial growth in a porous medium.

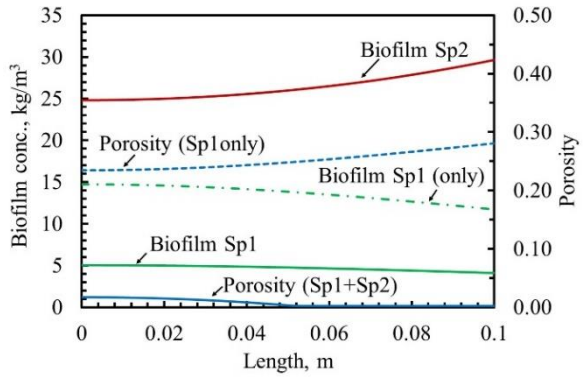

Figure 4. Profiles of biofilm concentration and porosity along the length of the medium at the end of the simulation. *Solid-lines* and *dashed-lines* represent "both species" and "single species" simulations, respectively.

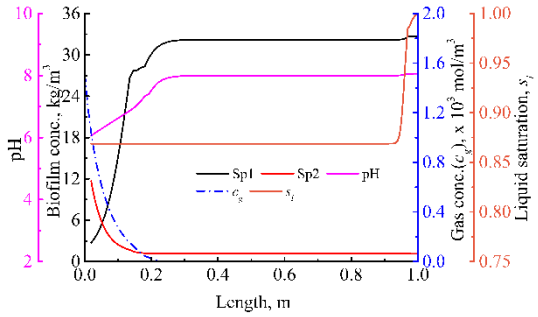

Figure 5. Profiles of Sp1 & Sp2 biofilm concentrations, pH, gas concentration (c_g), liquid saturation (s_l), along the length of the sandstone sample at the end of the two-phase flow simulation. Both species were considered in this simulation. Runtime 24 hrs.

The results show significant impacts of pH on biofilm growth. The results suggest that applications of biofilms as bio-barriers would be beneficial, if a combination of bacterial species that remains active over a wide pH range is used. In subsurface condition, naturally or due to anthropogenic activities such as carbon sequestration, pH may vary widely. In such scenarios a mono species biofilm that is active at specific pH values or in narrow pH ranges might be ineffective. Therefore, questions the usage of bio-barrier in engineering applications. In a mixed-species biofilm, certain species may become dormant at particular pH, but the other species can grow and contribute/participate to maintain barrier performance.

Conclusions

Within the limited scope of this paper, a study has been carried out to investigate the effect of pH on biofilm growth and the consequent impacts on porosity reduction. The effect of pH on a medium containing either a mixed species biofilm or a mono-species biofilm has been observed over a dynamic pH condition. The results suggest that a mixed bacterial species biofilm that covers a wide range of pH activity would be ideal for bio-barrier applications. Otherwise, if a single species is chosen which is active within a specific pH range will be dormant if the pH is not in favour. In such circumstances, the efficiency and usage of biofilm as bio-barriers might not be feasible or the efficiency of the barrier systems would be significantly lower than expected.

Acknowledgments

Funding to support this research was provided by Welsh Government and HEFCW through Ser Cymru National Research Network for Low Carbon, Energy and the Environment (NRN-LCEE) via Geo-Carb-Cymru Cluster.

References

[1] Bakke, R., *Biofilm detachment*, PhD Thesis, Montana State University, 1986, USA.

[2] Beyenal, H., Chen, S.N. & Lewandowski, Z., The double substrate growth kinetics of Pseudomonas aeruginosa, *Enzyme Microb. Technol.*, **32**, 2003, 92-98.

[3] Dixon, M. & Webb, E.C., *Enzymes*, Longman, 1979, London.

[4] Fredlund, D.G. & Rahardjo, H., *Soil Mechanics for Unsaturated Soils*, John Wiley & Sons Inc, 1993, New York.

[5] Hoštacká, A., Čižnár, I. & Štefkovičová, M., Temperature and pH Affect the Production of Bacterial Biofilm, *Folia Microbiol*, 55(1), 2010, 75-78.

[6] Ibragimova, S.I., Nerova, N.M. & Rabotnova, I.L., Kinetics of growth inhibition in Propionibac shermanii by hydrogen and hydroxyl ions, *Microbiol.*, **38**, 1969, 799-802.

[7] Masum, S.A. & Thomas, H.R., Modelling coupled microbial processes in the subsurface: Model development, verification, evaluation and application, *Adv. Water Resour.*, **116**, 2018, 1-17.

[8] Mitchell, A.C., Phillips, A.J., Hiebert, R., Gerlach, R., Spangler, L.H. & Cunningham, A.B., Biofilm enhanced geologic sequestration of supercritical CO_2, *Int. J. Greenh. Gas con.*, **3**(1), 2009, 90-99.

[9] Peyton, B.M., Effects of shear stress and substrate loading rate on Pseudomonas aeruginosa biofilm thickness and density, *Water Res.*, **30**(1), 1995, 29-36.

[10] Phillips, A.J., Gerlach, R., Lauchnor, E., Mitchell, A.C., Cunningham, A.B. & Spangler, L., Engineered applications of ureolytic biomineralization: a review, *Biofouling*, **29**(6), 2013, 715-733.

[11] Segel, I.H., *Enzyme kinetics: behavior and analysis of rapid equilibrium and steady-state enzyme systems*, Wiley-Interscience, 1975, New York.

[12] Sander, R., Compilation of Henry's law constants (version 4.0) for water as solvent, *Atmos. Chem. Phys.*, **15**, 2015, 4399-4981.

[13] Taylor, S.W. & Jaffé, P.R., Substrate and biomass transport in a porous medium, *Water Resour. Res.*, **26**(9), 1990, 2181–2194.

[14] Tan, Y., Wang, Z. & Marshall, K.C., Modelling pH Effects on Microbial Growth: A Statistical Thermodynamic Approach, *Biotechnol. Bioeng*, **59**, 1998, 724-731.

[15] Tang, I.C., Okos, M.R. & Yang, S.T., Effects of pH and acetic acid on homoacetic fermentation of lactate by *Clostridium formicoaceticum*, *Biotechnol. Bioeng.*, **34**, 1989, 1063-1074.